J Bioenerg Biomembr (2013) 45:511–518
DOI 10.1007/s10863-013-9521-0

Crystal structure of shrimp arginine kinase in binary complex with arginine—a molecular view of the phosphagen precursor binding to the enzyme

Alonso A. López-Zavala · Karina D. García-Orozco · Jesús S. Carrasco-Miranda · Rocio Sugich-Miranda · Enrique F. Velázquez-Contreras · Michael F. Criscitiello · Luis G. Brieba · Enrique Rudiño-Piñera · Rogerio R. Sotelo-Mundo

Received: 13 March 2013 / Accepted: 3 July 2013 / Published online: 20 July 2013

Abstract Arginine kinase (AK) is a key enzyme for energetic balance in invertebrates. Although AK is a well-studied system that provides fast energy to invertebrates using the phosphagen phospho-arginine, the structural details on the AK-arginine binary complex interaction remain unclear. Herein, we determined two crystal structures of the Pacific whiteleg shrimp (*Litopenaeus vannamei*) arginine kinase, one in binary complex with arginine (*Lv*AK-Arg) and a ternary transition state analog complex (TSAC). We found that the arginine guanidinium group makes ionic contacts with Glu225, Cys271 and a network of ordered water molecules. On the zwitterionic side of the amino acid, the backbone amide nitrogens of Gly64 and Val65 coordinate the arginine carboxylate. Glu314, one of proposed acid–base catalytic residues, did not interact with arginine in the binary complex. This residue is located in the flexible loop 310–320 that covers the active site and only stabilizes in the *Lv*AK-TSAC. This is the first binary complex crystal structure of a guanidine kinase in complex with the guanidine substrate and could give insights into the nature of the early steps of phosphagen biosynthesis.

Keywords Arginine kinase · Binary complex · Phosphagen · Crystal structure · Shrimp · *Litopenaeus vannamei*

A. A. López-Zavala · K. D. García-Orozco · J. S. Carrasco-Miranda · R. Sugich-Miranda · R. R. Sotelo-Mundo (✉)
Centro de Investigación en Alimentación y Desarrollo, A.C. (CIAD). Carretera a Ejido La Victoria Km 0.6, Apartado Postal 1735, Hermosillo, Sonora 83304, Mexico
e-mail: rrs@ciad.mx

R. Sugich-Miranda · E. F. Velázquez-Contreras · R. R. Sotelo-Mundo
Departamento de Investigación en Polímeros y Materiales (DIPM), Universidad de Sonora, Blvd. Luis Encinas y Rosales S/N, Col. Centro, Hermosillo, Sonora 83000, Mexico

M. F. Criscitiello
Comparative Immunogenetics Laboratory, Department of Veterinary Pathobiology, College of Veterinary Medicine and Biomedical Sciences, Texas A&M University, College Station, TX 77843, USA

L. G. Brieba
Laboratorio Nacional de Genómica para la Biodiversidad (LANGEBIO), Centro de Investigación y Estudios Avanzados (CINVESTAV) Km 9.6 Libramiento Norte Carretera Irapuato-León, Irapuato Guanajuato, 36500, Mexico

E. Rudiño-Piñera (✉)
Departamento de Medicina Molecular y Bioprocesos, Instituto de Biotecnología (IBt), Universidad Nacional Autónoma de México (UNAM), Av. Universidad #2001, Col. Chamilpa, Cuernavaca, Morelos 62250, Mexico
e-mail: rudino@ibt.unam.mx

Introduction

Under certain physiological situations in which fast energy production is required, phosphagens support cellular activity until catabolic pathways such as glycolysis and oxidative phosphorylation are turned on to replenish ATP levels (McGilvery and Murray 1974; Wallimann et al. 1992; Yousef et al. 2002). Phosphagens, such as phosphoarginine (in invertebrates) and phosphocreatine (in vertebrates) play an important role as "energy storage" molecules due to their highly energetic phosphate moiety that can be rapidly transferred to ADP when there is a sudden cellular requirement for ATP (Ellington 2001).

Arginine kinase (EC 2.7.3.3) (AK) plays an important role in invertebrate physiology by buffering the ATP pool accordingly to cellular energy requirements (Fig. 1). AK and its vertebrate

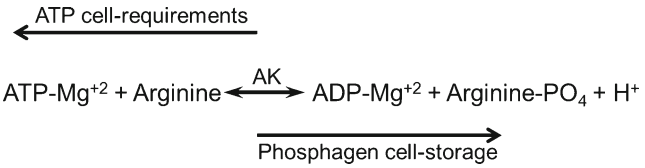

Fig. 1 The reversible reaction catalyzed by AK. In the forward reaction, AK synthetizes phosphagens for energy-cell storage. Under rapid cellular-energy requirements, AK hydrolyzes the phosphagen to supply the ATP cellular necessities, backward direction

homolog creatine kinase (CK) belong to the guanidine kinase (GK) family (Stroud 1996). Although there are structural variations in their substrates, all GK family members have a guanidine group as the final phosphate acceptor (Ellington 2001). AK has been isolated from multiple sources as a monomeric 40 kDa protein, and in some cases as an homodimer of approximately 80 kDa (Guo et al. 2003; Wu et al. 2010; Shi et al. 2012). Several biochemical, kinetic and structural data indicate that the detailed AK catalytic mechanism consists of a reversible, direct, in-line phosphate transfer between ATP and the arginine-guanidine group (Ellington 2001). Arginine and ATP bind randomly to the active site and products are individually released with a rapid equilibrium of enzyme:substrate and enzyme:product complexes (Blethen 1972).

Crystal structures of GKs from several sources have been reported: dimeric CK from human muscle (PDB entry 3B6R), Pacific electric ray (*Torpedo californica*, PDB entry 1VRP), and cytosolic bovine retinal-type CK (PDB entry 1G0W) (Tisi et al. 2001; Lahiri et al. 2002; Bong et al. 2008); as well as dimeric AK from sea cucumber (PDB entry 3JU6) (Wu et al. 2010), and monomeric AK from *Trypanosoma cruzi* (PDB entry 2J1Q) (Fernandez et al. 2007), horseshoe crab, *Limulus polyphemus* (PDB entry 1BG0) (Zhou et al. 1998) and recently, the white shrimp *Litopenaeus vannamei* (PBD entry 4 AM1) (Lopez-Zavala et al. 2012). Monomeric AK contains 357 amino acid residues comprising two domains: a small N-terminal domain of ~100 residues arranged in an irregular array of 6 short α-helices, and a larger C-terminal domain (~250 residues) formed by an alpha-beta two-layer sandwich fold consisting of a central core of an eight-stranded antiparallel β-sheet flanked by seven α-helices (Zhou et al. 1998). The *Limulus polyphemus* AK (*Lp*AK) crystal structure, forming a ternary state analog complex (TSAC) bound to ADP-Mg^{+2}, arginine and a nitrate ion, showed that when both substrates bound the AK active site, a conformational change occurred in loop 309–321 leading to a "closed ternary complex" (PDB entry 1BGO). This loop is located in the larger C-terminal domain and "covers" the active site as a lid, providing active site stabilization, substrate alignment, and avoiding wasteful ATP hydrolysis during catalysis (Zhou et al. 1998). Moreover, in the substrate-free enzyme *Lp*AK, known as the "open" form, this loop is disorganized and it is not visible in electron density maps. This observation is consistent with other AK structures in the open form, including AK from Pacific white shrimp (PDB entry 4 AM1) and *T. cruzi* (PDB entry 2J1Q). Meanwhile, the loop 59–64 located in the small domain is always ordered and it has been implicated in guanidine substrate specificity via hydrogen bridges from the backbone-loop to the arginine-carboxylate group (Zhou et al. 1998).

The structure of AK in a TSAC shows that precise pre-alignment of substrates contribute to catalysis (Zhou et al. 1998; Yousef et al. 2002). Therefore, local and global conformational changes in the entire molecule occur when the active site is fully occupied by the substrates (Zhou et al. 1998; Lahiri et al. 2002). However, lombricine kinase from *Urechis caupo* (*Uc*LK) crystal structure in complex with ADP (without Mg^{2+}) showed minimal conformational changes when compared to the substrate-free form (root mean square deviation r.m.s.d.=0.54 Å) (Bush et al. 2011).

Small-angle X-ray scattering (SAXS) experiments provided additional information about overall conformational changes to both AK and CK that occur upon nucleotide-Mg^{2+} binding. Similar results were reported by Liu et al. by intrinsic fluorescence emission spectra in AK from *Metapenaeus ensis* (greasyback shrimp) when nucleotide interacts with the enzyme (Liu et al. 2011). Also, SAXS studies showed only small global changes when guanidine substrate (arginine or creatine) binds to the active site (Dumas and Janin 1983; Forstner et al. 1998).

Structural work with GKs has focused on nucleotide binding and TSAC complexes. As mentioned before, AK and other GKs catalyze bi-substrate random-ordered reactions. Therefore, the binding of guanidine-substrate is also important but remarkably less studied. Structural solution studies revealed that only small global changes occur upon arginine binding (Dumas and Janin 1983; Forstner et al. 1998). Atomic details of arginine interactions alone with AK active sites have not been described to date. Actually, there are no available structural reports in the Protein Data Bank related to the AK (or other GKs) in binary complex with the substrate arginine.

Previously, we reported the purification, enzymatic activity (Garcia-Orozco et al. 2007) and crystallization of the marine shrimp *Litopenaeus vannamei* AK (*Lv*AK) without any ligands (open form) (Lopez-Zavala et al. 2012). AK has been studied from several crustacean species, with high amino acid sequence identity among them (>70 %). Biochemical and proteomic studies have found that *Lv*AK is up regulated during the shrimp immune response mechanisms against viral infection and in response to pattern recognition molecules representative of bacteria and yeast such as peptidoglycan and laminarin (Rattanarojpong et al. 2007; Yao et al. 2009). Interestingly, the β-subunit of the shrimp ATP synthase (Muhlia-Almazan et al. 2008; Martinez-Cruz et al. 2011) physically interacts with capsid proteins of the white spot

syndrome virus (Liang et al. 2010; Zhan et al. 2013), suggesting that a connection between the innate immune response of this crustacean and the bioenergetics machinery exists.

In this paper we report the crystallization and three-dimensional structure determination of *Lv*AK in a binary complex with the substrate arginine (*Lv*AK-Arg) at 1.9 Å resolution and "closed" form (*Lv*AK-TSAC) at 1.6 Å resolution. To the best of our knowledge, this is the first crystal structure of a GK in binary complex with the guanidine substrate. On the other hand, the overall structure of *Lv*AK-Arg is more similar to ligand-free apo-*Lv*AK than TSAC crystal structure. This *Lv*AK-Arg crystal structure will provide information towards understanding how AK binds the guanidine substrate in the first catalytic stages.

Experimental procedures

LvAK purification and crystallization of the binary LvAK-Arg complex and LvAK-TSAC

The *Lv*AK was purified from white shrimp abdominal muscle as previously reported (Garcia-Orozco et al. 2007). *Lv*AK purity was verified by the presence of a single band (~40 kDa) in silver-stained SDS-PAGE. The *Lv*AK activity was measured with a direct colorimetric assay in the forward direction detecting the synthesis of arginine phosphate (Yu et al. 2002). For crystallization trials, *Lv*AK was extensively dialyzed against 10 mM Tris–HCl pH 8.0, 1 mM DTT and concentrated with a 10-kDa ultrafiltration membrane (Amicon, Millipore, USA) to 20 mg/mL.

The *Lv*AK-Arg binary complex was obtained by incubating *Lv*AK with 4 mM *L-arginine* for 30 min at 4 °C before crystallization trials. Successful crystallization experiments were prepared using the micro batch method in Greiner plates (BioOne, USA) and solution #28 from the Crystal Screen I kit (Hampton Research, USA). The plates were prepared setting on each well 1 μL *Lv*AK-Arg binary complex mixed with 1 μL of the crystallization solution #28 (0.2 M sodium acetate, 0.1 M sodium cacodylate pH 6.5 and 30 % (w/v) PEG 8000), then 10 μL paraffin oil was added to cover the drop. The plates were incubated at 16 °C and the crystals grew after 3 weeks to a size of 0.35×0.2×0.15 mm. The *Lv*AK (20 mg/mL) was co-crystallized with several reagents to form the TSAC: ADP 16 mM, $MgCl_2$ 20 mM, *L*-arginine 40 mM and $NaNO_3$ 75 mM (all from Sigma-Aldrich, Mexico). The complex *Lv*AK-TSAC was incubated for 30 min at 4 °C before the crystallization droplets were prepared. The crystals were obtained by vapor diffusion using the hanging drop method in 24-well Limbro plates (Hampton Research, USA). The drop was setup by mixing 2 μl of *Lv*AK-TSAC with 2 μl of solution #28 from crystal screen I kit (Hampton Research). 0.5 mL solution # 28 were added to the well, sealed with vacuum grease and stored at 16 °C. Crystals were grown as large square bars which were broken to small crystals (0.1×0.1×0.3 mm) using an acupuncture needle.

Before cryo-cooling, the crystal was transferred to a cryoprotectant solution (Milli-Q water and PEG 8000 in the mother liquor were replaced with 30 % (v/v) PEG 400). Each single crystal was soaked in the cryoprotectant solution for 5 min, and then it was loop-mounted and flash-cooled under liquid nitrogen (100 K). For cryo-cooling of *Lv*AK-TSAC crystals, all ligands (ADP, $MgCl_2$, *L*-arginine and $NaNO_3$) were added to the cryoprotectant solution to give the same final concentration as in the crystallization drop.

X-ray data collection, phase solving and crystal structure determination

Data collection was performed on beamline X6A of the National Synchrotron Light Source (NSLS), Brookhaven National Laboratory (BNL, Upton, NY, USA), using an ADSC Quantum 270 detector. X-ray diffraction data were collected from single crystals at −0.9795 Å (12672 eV) and 0.9184 Å (13500 eV) (Table 1). The crystal-to-detector distance was kept at 200 mm and 230 mm (for *Lv*AK-TSAC and *Lv*AK-Arg, respectively) with an oscillation range per image of 0.5 °. The crystals were exposed for 5 s for *Lv*AK-TSAC, and for 10 s for *Lv*AK-Arg to the beam under a nitrogen stream at 100 K. Data sets were analyzed using XDS (Kabsch 2010) and SCALA softwares from the Collaborative Computational Project Number 4 (CCP4) (Winn et al. 2011). The *Lv*AK-Arg crystal belonged to the $P2_12_12_1$ space group, with unit-cell parameters a=56.4 Å, b=70.4 Å, c=82.1 Å. Matthews's coefficient calculations indicated that there was one molecule per asymmetric unit (V_M=2.03 $Å^3$ D^{-1}, 39.5 % of solvent content) (Matthews 1968). Data analysis of the *Lv*AK-TSAC crystal showed that it belongs to the $P2_1$ space group with unit-cell parameters a=63.3 Å, b=67.2 Å, c=78.8 Å, β=92.1° and a Matthews's coefficient parameters of V_M=2.09 $Å^3$ D^{-1} and 41.2 % of solvent content. These calculations are in accordance with two molecules per asymmetric unit. Data-collection statistics are listed in Table 1. Phases for *Lv*AK-Arg and *Lv*AK-TSAC sets were determined by molecular replacement in PHASER (McCoy et al. 2005), using the *Lv*AK (PDB entry 4 AM1) coordinates previously determined by our group (Lopez-Zavala et al. 2012) and the horseshoe crab TSAC complex *Lp*AK (PDB entry 1 M10) (Zhou et al. 1998) as search molecules, respectively. Refinement was performed using several cycles comprising the programs PHENIX (Adams et al. 2010) and COOT for manual building (Emsley et al. 2010).

Table 1 Data reduction and refinement statistics from binary and ternary AK structures. Values in parenthesis represent the statistics at the highest resolution bin

Data set	*Lv*AK-Arg	*Lv*AK-TSAC
X-ray source	NSLS X6A	NSLS X6A
Detector	Quantum 270 CCD	Quantum 270 CCD
Wavelength (Å)	0.9795 Å	0.9184 Å
Space group	$P2_12_12_1$	$P2_1$
Unit-cell parameters (Å)	a=56.4, b=70.4, c=82.1	a=63.3, b=67.2, c= 78.8; β=92.1°
Number of residues	356	712
Monomers per asymmetric unit	1	2
Mathews coefficient (Å Da^{-1})	2.03	2.00
Solvent content (%)	39.5	41.2
Resolution range (Å)	19.1–1.9 (2.01–1.9)	14.8–1.6 (1.7–1.6)
Total reflections	189,792 (28,192)	325,408 (51,061)
Unique reflections	26,516 (4060)	86,195 (13,556)
R_{symm} [a]	0.060 (0.198)	0.049 (0.281)
R_{meas} [b]	0.065 (0.213)	0.057 (0.328)
Completeness (%)	100 (96.1)	99.1 (98.2)
$I/\sigma(I)$	22.3 (5.4)	20.9 (4.9)
Wilson plot B value	15.15	11.73
Redundancy	7.1 (6.9)	6.3 (6.3)

[a] $R_{symm}=\sum_{hkl}\sum_i|I_i(hkl)-(I(hkl))|/\sum_{hkl}\sum_i I_i(hkl)$, where $I_i(hkl)$ and $(I(hkl))$ represent the diffraction-intensity values of the individual measurements and the corresponding mean values. The summation is over all unique measurements

[b] R_{meas} is a redundancy-independent version of R_{symm}, $R_{meas}=\sum_h\sqrt{n_h/n_h-1}\sum^{nh}{}_i|\hat{I}_h-I_{h,i}|/\sum_h\sum^{nh}{}_i I_{h,i}$, where $\hat{I}_h-1/n_h\sum^{nh}{}_i I_{h,i}$

Results and discussion

Analysis of guanidine binding site in LvAK-Arg crystal structure

The AK catalytic mechanism has been extensively described by classical methods (Blethen 1972). AK is one of most studied enzymes of the GK family; these enzymes have a bi-substrate random mechanism for transferring a γ- phosphate group between ATP and the guanidine end of arginine. Each side of this reversible reaction has different physiological functions, in one direction to produce phosphagen (phosphoarginine) energy stores and in the other direction to use it for ATP synthesis (Fig. 1). Each substrate has an independent binding site that through a strong conformational change in the entire molecule comes close together to facilitate the reaction (Zhou et al. 1998). Several crystal structures of AKs both free and fully occupied by ligands have been reported. A few reports of other members of the GK family are in a binary complex with ADP-Mg^{+2} showing minimal conformational changes that are crucial for catalysis (Bong et al. 2008; Bush et al. 2011). However, there is hardly any structural work related to binding of arginine in AK (Dumas and Janin 1983; Forstner et al. 1998).

Crystal structures reported here shows the *Lv*AK in a binary complex with arginine at 1.9 Å resolution and in a ternary complex with ADP-Mg^{+2}, nitrate and arginine at 1.6 Å resolution that represents the ternary transition state analog complex (TSAC) (Tables 1 and 2). The overall *Lv*AK-Arg crystal structure shows a canonical AK folding with an α-helical N-terminal domain and a α-β C-terminal domain, the active site is located between both domains (Fig. 2a). Interestingly, the *Lv*AK binary complex shows a typical "open" conformation as in the apo-*Lv*AK (Lopez-Zavala et al. 2012). A superposition between both structures indicates no significant changes between them (r.m.s.d=0.20 Å for the C-α atoms) (Fig. 2a). Likewise, the *Uc*LK crystal structure bound to ADP-Mg^{+2} suffers little conformational changes related to the unbound substrate-free form (r.m.s.d.=0.54 Å considering only the C-α atoms) (Bush et al.

Table 2 Refinement statistics

Data set	*Lv*AK-Arg	*Lv*AK-TSAC
$R_{work}/R_{free(5\%)}$	0.1666/0.2155	0.1889/0.2157
Content of asymmetric unit		
Protein atoms	2850	5784
Ligands	12	88
Water molecules	314	599
R.M.S.D. form ideal		
Bond length (Å)	0.006	0.007
Bond angles (°)	0.998	1.208
Mean overall B value ($Å^2$)		
Protein	14.29	15.20
Solvent	39.85	18.20
Ramachandran plot, residues in		
Most favored regions	348(98 %)	690 (97.0 %)
Additionally allowed regions	5(1.43 %)	12 (1.8 %)
Outliers	2(0.57 %)	8 (1.1 %)
PDB code	4BHL	4BG4

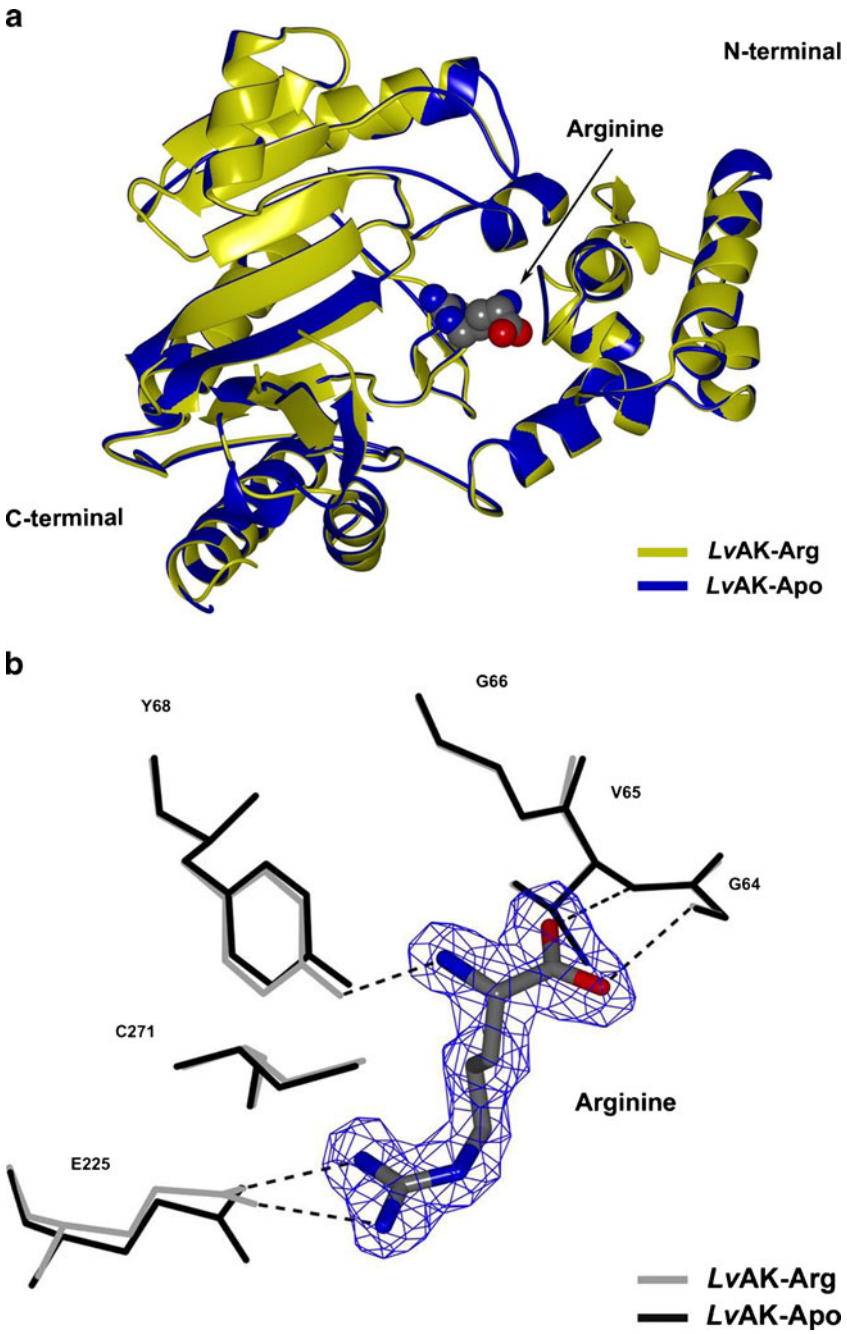

Fig. 2 Crystallographic structures free-ligand and arginine-complex *Lv*AK. **a** Superposition of binary complex (*yellow*) and the free substrate of *Lv*AK (*blue*). No conformational changes in overall structure were found after arginine binding (rmsd=0.26 Å). The guanidine substrate arginine is shown as spheres and colored by element. **b** The substrate arginine is well stabilized via hydrogen bonds throw the guanidine-binding loop (residues 64–66). *Lv*AK-Arg is shown in grey and apo-*Lv*AK in black, both as wide bonds. Glu224 is aligned toward the guanidine end of Arginine substrate (cylinders). Hydrogen bonds are shown as a dotted line using *Lv*AK-Arg structure as reference. Arginine electron density is displayed as a blue mesh in a 2Fo-Fc map at 2.5σ contour

2011). Also, the dimeric *Torpedo californica* creatine kinase (*Tc*CK) crystal structure bound to ADP-Mg^{+2} was obtained in the same crystal as TSAC. These results show that *Tc*CK nucleotide complex has an open conformation and that the residues involved in nucleotide binding did not change in relation to the *Tc*CK closed form (Lahiri et al. 2002).

GKs have different substrate specificities, which are diverse in structural and physicochemical properties. In all GKs, the guanidine-binding loop is located in the N-terminal domain and it has been proposed that the loop length is inversely correlated with substrate size. GKs with a small loop bind the largest guanidine substrate (Azzi et al. 2004). *Lv*AK has high amino acid sequence identity (≈70 %) related to other monomeric AKs, and a well-conserved guanidine-binding loop comprised from residues 59 to 64. Figure 2b depicts a superposition of *Lv*AK binary complex (black) and apo-*Lv*AK (gray) residues that comprise the guanidine-binding site.

The *Lv*AK-Arg structure shows that the substrate arginine is stabilized via backbone hydrogen bonds (Gly64, Val65 and Gly66) to the carboxylate moiety and from the hydroxyl of Tyr68 to the substrate amino group (Fig. 2b). Gly66 backbone hydrogen bond is not shown. This result is consistent with the previously determined *Lp*AK structure in the closed form in which the active site is filled with all the

ligands in the ternary analog complex (Zhou et al. 1998). Cys271 is another highly conserved residue that has been shown catalytic important as noted by chemical modification with sulfhydryl-specific reagents performed by Marletta and Kenyon and others authors (Marletta and Kenyon 1979; Buechter et al. 1992; Furter et al. 1993). This residue was found in the same orientation in both *Lv*AK complexes reported here (Figs. 2b and 3b). Also, Glu225 is one of the two bases (along with Glu314) involved as catalytic acid–base assisting the nucleophile attack for phosphate transfer.

Besides, these two residues are directly implicated in precise substrate guanidine-end alignment toward the nucleotide phosphate group during catalysis (Pruett et al. 2003). Surprisingly, in the *Lv*AK-Arg structure almost all residues in the guanidine-binding site are in the same position as in the free-ligand of *Lv*AK structure, except the Glu225 side chain that is slightly rotated to be positioned perfectly towards the arginine guanidine-end via ionic bonds (Fig. 2b). Pruett et al. mutated this residue to Asp and Gln in *Lp*AK to study the acid–base contribution during catalysis (Pruett et al. 2003). Crystal structures and enzymatic kinetic studies of these mutants show that the mutant enzymes have significantly less residual enzymatic activity (2–3 orders of magnitude) relative to the native *Lp*AK and subtle

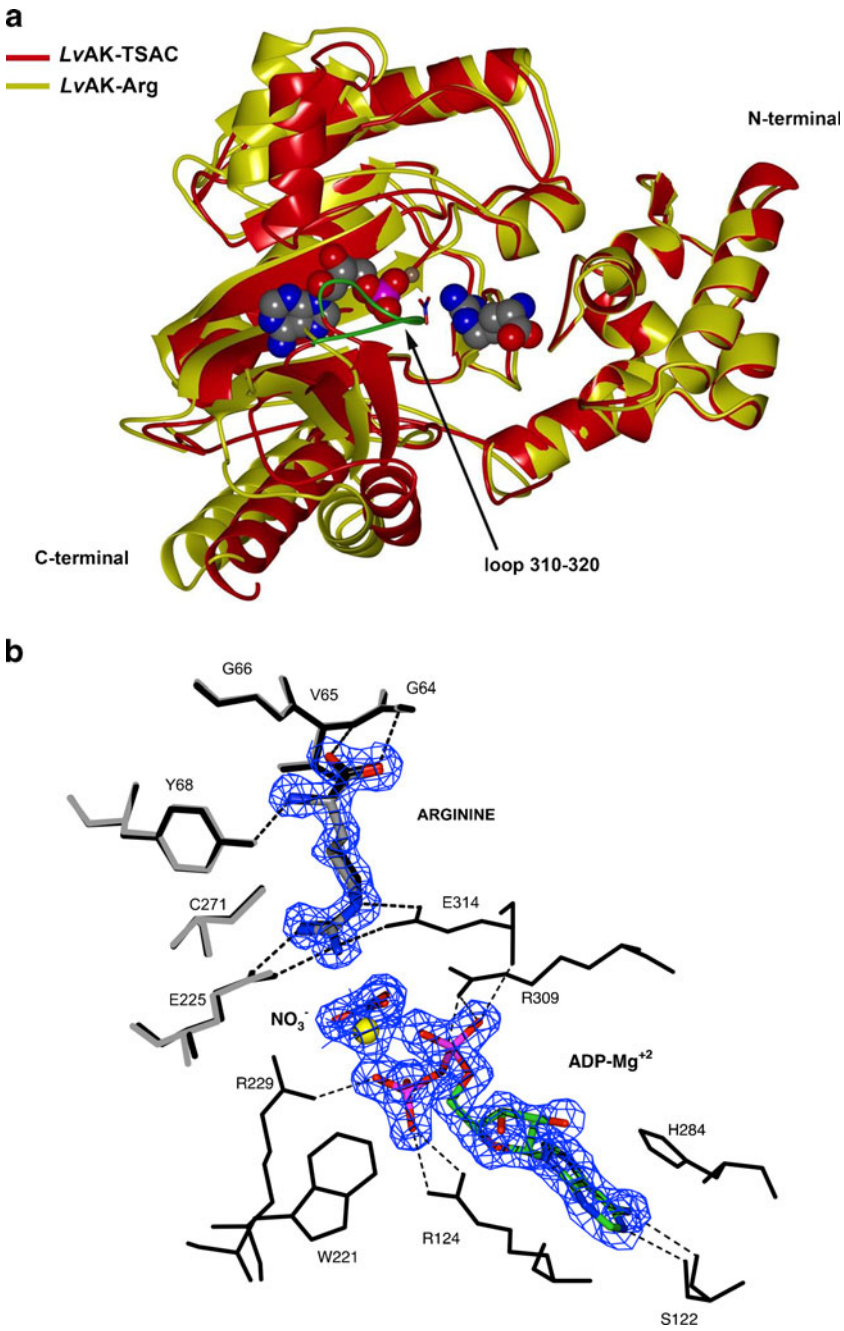

Fig. 3 **a** Superposition of *Lv*AK-Arg binary (*yellow*) and *Lv*AK-TSAC (*red*) crystal structures. In the guanidine-substrate binary complex loop 310–320 was disordered as in the "open form" of the enzyme. This loop is stabilized in the closed form of *Lv*AK-TSAC and serves as a "lid" to the active site (shown in *green*). ADP-Mg^{++} and Arginine are shown as spheres and nitrate ion as cylinders, all they are colored by element. **b** The arginine-binding site did not show substantial conformational changes when substrates occupy the active site in *Lv*AK-TSAC (*black*) when compared with *Lv*AK-Arg (*grey*). Except, Glu314 (wide bonds) stabilize and align the arginine (cylinders colored by element) guanidine-end to the nitrate ion (cylinders) that mimics the γ-phosphate of ATP in *Lv*AK-TSAC. Substrates coordinates belong to the *Lv*AK-TSAC. Arginine in the binary complex is presented as black cylinders. Hydrogen bonds are shown as a dotted line. *Lv*AK-TSAC Arginine electron density is displayed as a blue mesh in a 2Fo-Fc map at 3σcontour. The electron density and surrounding residues for the ADP-Mg^{++} are also shown. Magnesium ion is shown as a yellow sphere

perturbations of 5–14° toward the phosphagen guanidine-end. Substrate pre-alignment could be the most important role of Glu225 to facilitate the phosphate transference mediated by AK (Pruett et al. 2003). *Lv*AK-Arg structure shows that in the binary guanidine intermediate, small local conformational changes take Glu225 to its catalytic final position as in the enzyme ternary analog complex (Fig. 3b).

In comparison with the other two *Lv*AK structures, the *Lv*AK-TSAC has significant differences, most drastically an overall closing towards the substrates. This is clearly shown when the binary *Lv*AK-Arg (Fig. 3a, yellow) and the *Lv*AK-TSAC (Fig. 3a, red) complexes were superimposed using the N-terminal (residues 1–99, r.m.s.d=1.40 Å for the C-α atoms) as fixed domain (Fig. 3a). Changes were observed in almost the entire C-terminal domain (residues 100–356), which orients both substrates in close proximity favoring catalysis as in other AK structures (Zhou et al. 1998; Fernandez et al. 2007). In detail, major conformational movements were found in loop 310–319 (shown in green) since it positions over both substrates and serves as a "lid" to the enzyme active site. This loop is highly conserved in all monomeric AKs, *Lp*AK (GTRGEHTESE) and *Lv*AK (GTRGEHTEAE), and it is well ordered in crystallographic structures only when both substrates occupy the active site in the transition state complex (Zhou et al. 1998). Other kinases have similar conformational changes during nucleotide binding. Adenylate kinase is one well-studied example among the nucleoside monophosphate (NMP) kinase family (Randak and Welsh 2007; Daily et al. 2010).

Adenylate kinases, as other NMP kinases, consist of three typical domains related to nucleotide binding: the NMP-binding, the CORE and the LID domains. The LID domain is known to have the largest conformational change during nucleotide binding (~60 Å hinge bending) avoiding waste of energy during catalysis.

In AKs, Glu314 is located in loop 310–320 and it has been proposed as an important base during catalysis. This residue has interactions via salt bridge and hydrogen bond with the arginine guanidine-end, specifically with Arginine-N_{η} and $N_{\eta 2}$, respectively (Fig. 3b). Also, Glu314 positions the arginine guanidine-end in the right orientation toward the γ-phosphate of ATP (Pruett et al. 2003). However, in the binary *Lv*AK-Arg structure no electron density was observed for loop 310–320. Therefore, this loop is disordered and did not appear over the active site as in the *Lv*AK-TSAC. Similarly, the structure of *Tc*-CK bound to the nucleotide substrate in a binary complex did not show a well-ordered flexible loop (in CK residue Val325 is the homologous position to Glu314 in AK). This loop moves to the correct place only when the guanidine substrate is bound to the active site as in the transition state providing a binding pocket for creatine (Lahiri et al. 2002).

Similar experiments have been performed in other kinases from different protein families (hexokinase or phosphoglycerate kinase) (McDonald et al. 1979; Pickover et al. 1979). It was found from crystallographic studies of free ligand form and non-nucleotide substrate binary complex (glucose or 3-phosphoglicerate) that a large conformational change takes place in the entire molecule. In hexokinase, glucose binding results in a movement of up to 9 Å in one of the two domains and a closure of the glucose binding pocket (McDonald et al. 1979). In contrast, binding of Mg-nucleotide does not cause changes in the overall structure of these enzymes. As mentioned, in the *Lv*AK-Arg structure the loop 310–320 is disordered, therefore Glu314 was not visible in the binary-arginine complex crystal structure. Hence, this residue appears to be not essential for arginine binding to the *Lv*AK active site. Kinases avoid wasteful ATP hydrolysis by the mechanism of induced fit, which engages large conformational changes binding upon both substrates. This movements traps substrates and avoids the escape reaction intermediates (Koshland 1958; Knowles 1991).

Our findings are consistent with other previously reported GKs binary nucleotide complex structures suggesting that the binding of one substrate to the active site does not promote the loop 310–320 final catalytic position as in the ternary analog complex. Likewise, both SAXS studies and X-ray crystal structures findings of individual binding of either two substrates (3-phospohoglicerate and Mg-ATP) to phosphoglycerate kinase do not lead to substantial domain rearrangements. Only binding of both substrates promotes the complete conformational changes associated with catalysis (Harlos et al. 1992; Varga et al. 2006). The *Lv*AK-Arg structure shows arginine bound to the enzyme active site nearly in the same position as in the *Lv*AK-TSAC. The guanidine substrate is coordinated consistently in both reaction intermediates via hydrogen bonds with the backbone of residue Tyr68 of the guanidine specificity loop and salt bridges to Glu225. All of these residues did no show significant changes going from binary-open to ternary-closed form.

Conclusions

In this work we present a previously undescribed stage of the reaction mechanism of AKs. Interestingly, the overall structure of *Lv*AK-Arg is more similar to apo-*Lv*AK than to the ternary-closed form. Also, arginine binding to the AK active site does not causes global conformational changes. This is consistent with SAXS experiments performed by Dumas and Janin (1983) and in CK (Dumas and Janin 1983; Forstner et al. 1998 #18). Furthermore, The *Lv*AK-Arg structure shows in detail that upon arginine binding no major local conformational changes occur in the guanidine-binding site. Our findings together with other previously reported GK binary complex structures suggest that binding of one substrate to the active site does not promote the proper arrangement of loop 310–320 as in the ternary analog complex. Binding of both substrates appears to be strictly necessary

to achieve the appropriate AK conformational changes associated with catalysis. Future studies will allow a better understanding of the guanidine substrate interaction with the enzyme during the first reaction stages.

Acknowledgements R.R. Sotelo-Mundo and M.F. Criscitiello thank grant 2011–050 from the Texas A&M-CONACYT (Mexico's National Research Council for Science and Technology) Collaborative Grant Program and CONACYT grants CB-2009-131859 and E0007-2011-01-179940 and COFUPRO RNIIPA-2012-024 grant. A.A. López-Zavala and J.S. Carrasco-Miranda thank CONACYT for their doctoral fellowship. Dr. Sugich-Miranda was a postdoctoral fellow at Dr. Sotelo's Lab during this investigation, supported by Universidad de Sonora. We thanks Dr. Vivian Stojanoff and the staff at BNL NSLS beamline X6A for data-collection facilities. Beamline X6A is funded by NIGMS (GM-0080) and the US Department of Energy (No. DE-AC02-98CH10886). Dr. Sotelo-Mundo thanks support for a sabbatical leave at DIPM, Universidad de Sonora.

References

Adams PD, Afonine PV, Bunkoczi G, Chen VB, Davis IW, Echols N, Headd JJ, Hung LW, Kapral GJ, Grosse-Kunstleve RW, Mccoy AJ, Moriarty NW, Oeffner R, Read RJ, Richardson DC, Richardson JS, Terwilliger TC, Zwart PH (2010) Acta Crystallogr D: Biol Crystallogr 66:213–221

Azzi A, Clark SA, Ellington WR, Chapman MS (2004) Protein Sci 13:575–585

Blethen SL (1972) Arch Biochem Biophys 149:244–251

Bong SM, Moon JH, Nam KH, Lee KS, Chi YM, Hwang KY (2008) FEBS Lett 582:3959–3965

Buechter DD, Medzihradszky KF, Burlingame AL, Kenyon GL (1992) J Biol Chem 267:2173–2178

Bush DJ, Kirillova O, Clark SA, Davulcu O, Fabiola F, Xie Q, Somasundaram T, Ellington WR, Chapman MS (2011) J Biol Chem 286:9338–9350

Daily MD, Phillips GN Jr, Cui Q (2010) J Mol Biol 400:618–631

Dumas C, Janin JL (1983) FEBS Lett 153:128–130

Ellington WR (2001) Annu Rev Physiol 63:289–325

Emsley P, Lohkamp B, Scott WG, Cowtan K (2010) Acta Crystallogr D: Biol Crystallogr 66:486–501

Fernandez P, Haouz A, Pereira CA, Aguilar C, Alzari PM (2007) Proteins 69:209–212

Forstner M, Kriechbaum M, Laggner P, Wallimann T (1998) Biophys J 75:1016–1023

Furter R, Furter-Graves EM, Wallimann T (1993) Biochemistry 32:7022–7029

Garcia-Orozco KD, Aispuro-Hernandez E, Yepiz-Plascencia G, Calderon-De-La-Barca AM, Sotelo-Mundo RR (2007) Int Arch Allergy Immunol 144:23–28

Guo SY, Guo Z, Guo Q, Chen BY, Wang XC (2003) Protein Expr Purif 29:230–234

Harlos K, Vas M, Blake CF (1992) Proteins 12:133–144

Kabsch W (2010) Acta Crystallogr D: Biol Crystallogr 66:125–132

Knowles JR (1991) Philos Trans R Soc Lond B Biol Sci 332:115–121

Koshland DE (1958) Proc Natl Acad Sci U S A 44:98–104

Lahiri SD, Wang PF, Babbitt PC, Mcleish MJ, Kenyon GL, Allen KN (2002) Biochemistry 41:13861–13867

Liang Y, Cheng JJ, Yang B, Huang J (2010) Virol J 7:144

Liu N, Wang JS, Wang WD, Pan JC (2011) Int J Biol Macromol 49:98–102

Lopez-Zavala AA, Sotelo-Mundo RR, Garcia-Orozco KD, Isac-Martinez F, Brieba LG, Rudino-Pinera E (2012) Acta Crystallogr Sect F Struct Biol Cryst Commun 68:783–785

Marletta MA, Kenyon GL (1979) J Biol Chem 254:1879–1886

Martinez-Cruz O, Garcia-Carreno F, Robles-Romo A, Varela-Romero A, Muhlia-Almazan A (2011) J Bioenerg Biomembr 43:119–133

Matthews BW (1968) J Mol Biol 33:491–497

Mccoy AJ, Grosse-Kunstleve RW, Storoni LC, Read RJ (2005) Acta Crystallogr D: Biol Crystallogr 61:458–464

Mcdonald RC, Steitz TA, Engelman DM (1979) Biochemistry 18:338–342

Mcgilvery RW, Murray TW (1974) J Biol Chem 249:5845–5850

Muhlia-Almazan A, Martinez-Cruz O, Navarrete Del Toro Mde L, Garcia-Carreno F, Arreola R, Sotelo-Mundo R, Yepiz-Plascencia G (2008) J Bioenerg Biomembr 40:359–369

Pickover CA, Mckay DB, Engelman DM, Steitz TA (1979) J Biol Chem 254:11323–11329

Pruett PS, Azzi A, Clark SA, Yousef MS, Gattis JL, Somasundaram T, Ellington WR, Chapman MS (2003) J Biol Chem 278:26952–26957

Randak CO, Welsh MJ (2007) J Bioenerg Biomembr 39:473–479

Rattanarojpong T, Wang HC, Lo CF, Flegel TW (2007) Proteomics 7:3809–3814

Shi X, Wang L, Zhou Z, Yang C, Gao Y, Song L (2012) Dev Comp Immunol 37:270–278

Stroud RM (1996) Nat Struct Biol 3:567–569

Tisi D, Bax B, Loew A (2001) Acta Crystallogr D: Biol Crystallogr 57:187–193

Varga A, Flachner B, Konarev P, Graczer E, Szabo J, Svergun D, Zavodszky P, Vas M (2006) FEBS Lett 580:2698–2706

Wallimann T, Wyss M, Brdiczka D, Nicolay K, Eppenberger HM (1992) Biochem J 281(Pt 1):21–40

Winn MD, Ballard CC, Cowtan KD, Dodson EJ, Emsley P, Evans PR, Keegan RM, Krissinel EB, Leslie AG, Mccoy A, Mcnicholas SJ, Murshudov GN, Pannu NS, Potterton EA, Powell HR, Read RJ, Vagin A, Wilson KS (2011) Acta Crystallogr D: Biol Crystallogr 67:235–242

Wu X, Ye S, Guo S, Yan W, Bartlam M, Rao Z (2010) FASEB J 24:242–252

Yao CL, Ji PF, Kong P, Wang ZY, Xiang JH (2009) Fish Shellfish Immunol 26:553–558

Yousef MS, Fabiola F, Gattis JL, Somasundaram T, Chapman MS (2002) Acta Crystallogr D: Biol Crystallogr 58:2009–2017

Yu Z, Pan J, Zhou HM (2002) Protein Pept Lett 9:545–552

Zhan W, Wang X, Chi Y, Tang X (2013) Fish Shellfish Immunol 34:228–235

Zhou G, Somasundaram T, Blanc E, Parthasarathy G, Ellington WR, Chapman MS (1998) Proc Natl Acad Sci U S A 95:8449–8454